FLOW PATTERN PREDICTION & VALIDATION FOR DISCONTINUOUS PREPREG USING ANISOTROPIC VISCOUS FLOW SIMULATION

Anthony J. Favaloro, Drew E. Sommer, R. Byron Pipes
Composites Manufacturing and Simulation Center, Purdue University, West Lafayette, IN

Abstract

Carbon fiber prepreg cut and slit into rectangular platelets offer an intermediate material solution between continuous carbon fiber composites and short fiber molding composites. Prepreg platelet molding compounds (PPMCs), sometimes called carbon fiber SMC, can be used to mold moderately complex geometries while providing moderate mechanical performance. However, to understand the mechanical behavior of the final geometry, the orientation state of the reinforcing platelets must be known. Herein, we present an anisotropic viscous flow simulation coupled with orientation evolution for PPMCs. This simulation technique is applied to the molding of a double dome geometry with two different initial charge orientations. The simulation is validated through blind prediction of flow patterns that compare well to short shot experiment for both charge orientations. The resulting orientation states are analyzed and compared.

Introduction

In order to accurately describe the mechanical performance of fiber reinforced composites, the fiber orientation state must be known [1]. While high performance composites applications directly prescribe the fiber orientation state, high rate processes such as compression molding or injection molding contain flow induced orientation states [2]. Recently, a class of materials referred to as prepreg platelet molding compounds (PPMCs) has been introduced to serve as an intermediate material solution between continuous fiber composites and short fiber molding composites. PPMCs are formed by cutting and slitting pre-impregnated composite tape to a prescribed length and width while inheriting the thickness of the parent tape. The resulting platelets are then gathered into a mat. A photograph of an unconsolidated mat can be seen in Figure 1. Thus, the high fiber volume fraction obtained in the prepreg process is maintained in the molding material. Concurrently, an additional scale of interest is introduced (i.e. the platelet scale). The VORAFUSE™ M6400 material system by Dow is investigated in this work. The matrix material of the M6400 system is a fast curing thermoset enabling high rate manufacturing.

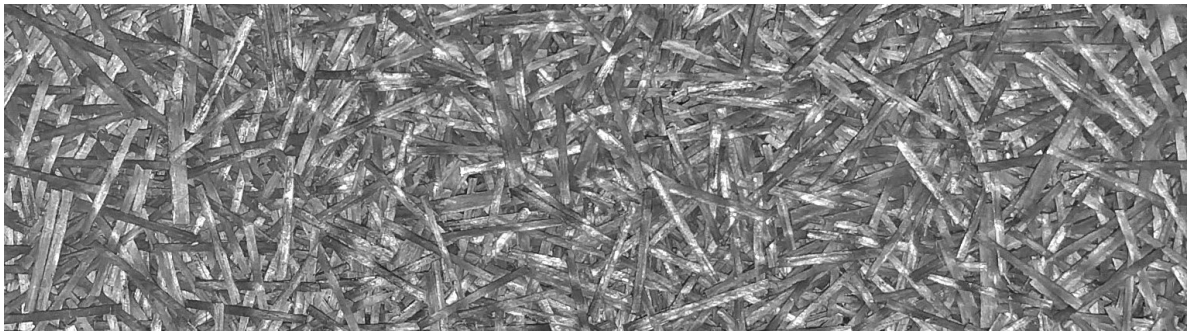

Figure 1: Photograph of Unconsolidated PPMC Mat

Herein, the double dome geometry and two initial charge orientations are investigated as shown in Figure 2. The physical manufacturing process involves:

- preparing the charge of material by cutting the PPMC mat to the appropriate dimensions and stacking a number of layers of mat to the desired weight
- preheating the tool, manual placement of the material into the charge cavity including by-hand forming of the material onto the tool contours
- closing the tool to a moderate clamping force to initiate efficient heat transfer for a short time allowing the viscosity of the thermosetting matrix to drop to the processing window
- applying large clamping force to flow the material to fill the cavity and holding the force until the material has cured.

In this way, the full manufacturing process represents a complex thermal, chemical, and rheological problem. Thus, the scope of this investigation is limited to modeling only the flowing stage of the process assuming the material has uniformly reached the processing window (i.e. the viscosity drop of the matrix material) and that the time scale of the molding is shorter than the time scale of the curing process. Under these assumptions, the process simulation is approached as *isothermal* with a *Newtonian* matrix viscosity but with *anisotropic* reinforcing effects of the fiber accounted for through a fully coupled anisotropic viscosity and *fiber orientation analysis* constitutive model. The simulation is applied to the double dome geometry with an initial transverse charge and an initial axial charge. The simulated flow patterns are compared to experimental short shots as an initial validation and the orientation state between simulation parts is compared. The simulations were performed prior to the experiments as a blind prediction.

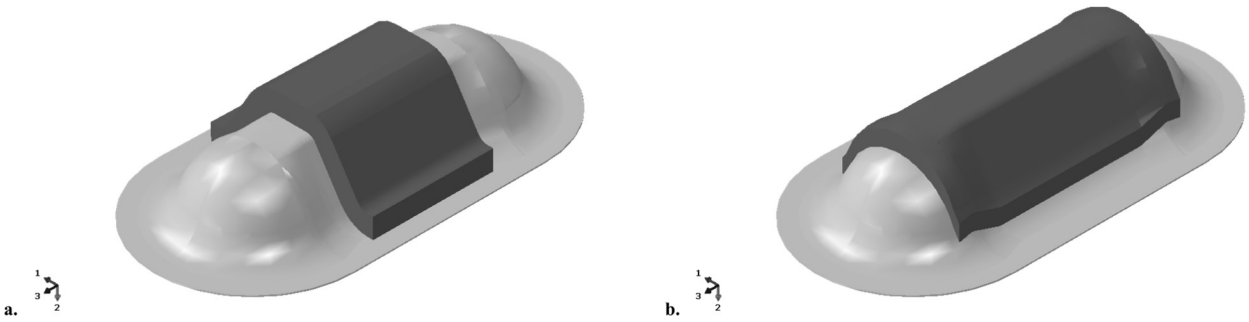

*Figure 2: Double Dome Geometry and Two Initial Charge Patterns: a. **Transverse** Charge, b. **Axial** Charge*

Theory and Implementation

In this work, the approach taken is of modeling the flow behavior of the PPMC charge using an anisotropic viscous constitutive relationship coupled with fiber orientation analysis. The constitutive model is implemented as a VUMAT in Abaqus/Explicit and the smoothed particle hydrodynamics method (SPH) method is used such that microstructural variable (i.e. fiber orientation) is tracked in a Lagrangian framework capable of extreme deformations [3,4]. In addition to the constitutive model, simulation model creation and initialization methods are developed to mirror the physical process of placing and forming the material in the tool by hand.

Fully Coupled Constitutive Model

Orientation analysis is a well-studied problem when concerning injection molding material systems. In the state of the art, Jeffery's equation [5] is expressed in a tensorial form as introduced by Advani and Tucker [6]. Next, a diffusion term, isotropic [7] or anisotropic [8–10], is added such that after large total strain an appropriate, non-collimated steady orientation structure is approached with anisotropy in diffusion introduced primary to prevent out-of-plane orientation to develop in thin structures. These simulations are typically performed neglecting anisotropy of the effective viscous fluid. For planar, glass mat thermoplastics (GMT) with large aspect ratio fibers, Ericsson et al. [11] demonstrated that the flow front of squeeze flow charges could be captured using affine motion for the fiber orientation model (i.e. Jeffery's equation with a shape factor of unity) and a coupled anisotropic constitutive model. The authors have previously reproduced the experimental results of Ericsson et al. using a finite element based approach in Abaqus/Standard [12]. Without sufficient experimental evidence to suggest the need for more complex fiber orientation models, the simplest possible model is adopted of affine motion. The local orientation structure of a platelet is described by three unit vectors as shown in Figure 3: the fiber direction, p, the transverse direction, q, and the normal direction, r. Limiting considerations to the fiber direction, affine motion gives the fiber orientation, p, after the material point has undergone a certain deformation gradient, F, from an initial orientation, p^0, as in Equation (1).

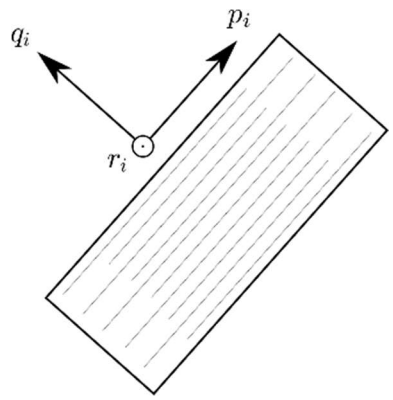

Figure 3: Platelet Coordinate System

$$p = \frac{\mathrm{F} \cdot p^0}{\|\mathrm{F} \cdot p^0\|} \tag{1}$$

The fiber orientation is then coupled to the viscous behavior through an orientation averaged transversely isotropic viscosity tensor [3,12], Equation (2), where A and $\mathbb{A}$ are the common second and fourth order orientation tensors [6], η_{23} is the isotropic shearing viscosity representing an increase over the matrix viscosity due to the presence of fibers, and $R_\eta = \eta_{11}/\eta_{22}$ is the anisotropy ratio representing the ratio of the resistance to extensional deformation along fiber axes versus transverse to fiber axes [13,14]. As the SPH method, an explicit method, is used to enable extreme deformation analyses the total stress tensor is expressed as in Equation (3) where K is a penalizing bulk modulus to enforce near incompressibility but allow for a non-zero stable time increment. In this work, $R_\eta = 116$ while the exact value of η_{23} is unimportant for flow pattern and orientation state predictions as it will simply scale the required force.

$$\langle\eta\rangle_{ijkl} = 4\eta_{23}(R_\eta - 1)\left[\mathbb{A}_{ijkl} - \frac{1}{3}\left(\mathrm{A}_{ij}\delta_{kl} + \mathrm{A}_{kl}\delta_{ij} - \frac{1}{3}\delta_{ij}\delta_{kl}\right)\right] + 2\eta_{23}\left[\frac{1}{2}\left(\delta_{ik}\delta_{jl} + \delta_{il}\delta_{jk}\right) - \frac{1}{3}\left(\delta_{ij}\delta_{kl}\right)\right] \quad (2)$$

$$\sigma_{ij} = \langle\eta\rangle_{ijkl}\dot{\epsilon}_{kl} + K(\det \mathrm{F} - 1)\delta_{ij} \quad (3)$$

In typical analyses, sheet molding compounds (SMC) are treated as isotropic materials. However, Dumont and coworkers have developed an anisotropic material model [15] for SMCs dependent upon the local normal direction of the tool. In carefully designed flow cases in which large orientation state changes are not encountered, this modeling simplification could be quite useful. The viscosity tensor of Equation (2) can be adapted to such a form by substituting the form of the second and fourth order orientation tensors for a planar, uniform orientation state as shown in Equations (4) and (5) where $\mathrm{M}_{ij} = n_i n_j$ is a second order tensor representing the local normal direction, n_i.

$$\mathrm{A}_{ij}^{\mathrm{2DUniform}} = \frac{1}{2}\left(\delta_{ij} - \mathrm{M}_{ij}\right) \quad (4)$$

$$\mathbb{A}_{ijkl}^{\mathrm{2DUniform}} = \frac{1}{8}\left[\left(\delta_{ij} - \mathrm{M}_{ij}\right)\left(\delta_{kl} - \mathrm{M}_{kl}\right) + \left(\delta_{ik} - \mathrm{M}_{ik}\right)\left(\delta_{jl} - \mathrm{M}_{jl}\right) + \left(\delta_{il} - \mathrm{M}_{il}\right)\left(\delta_{jk} - \mathrm{M}_{jk}\right)\right] \quad (5)$$

As an additional model consideration, the flow solution is computed with pure slip boundary conditions. This choice is motivated two-fold. First, due to the typical manufacturing approach of placing cool or room temperature material charges into preheated tooling, under these conditions the development of an apparently slip boundary conditions has been observed in SMC [16,17]. Additionally, Tucker observed in an orders of magnitude analysis that in the presence of large anisotropy and flat orientation states, apparent plug flow (slip) develops in narrow gaps [18]. Thus, as heat transfer and curing effects are not considered, a pure slip boundary condition is adopted.

Simulation Model Creation

The process of manually placing material charges into the tooling cavity is a source of difficulty for developing an accurate simulation as compared to highly controlled processes such as injection molding. For the transverse charge, the length of the charge was totally contained in a portion of the double dome geometry having only two dimensional complexity. For this case the creation of the initial charge domain was performed by simple geometric means, see Figure 4. However, the length of the axial charge extends into a portion of the double dome geometry that contains three dimension features. To form the initial domain for the axial charge, a simple elastic forming simulation was performed considering a quasi-isotropic material definition. The charge domain was then padded from the forming simulation results. The transverse charge domain contained 221,076 PC3D elements, while the transverse charge contained 287,335 PC3D elements.

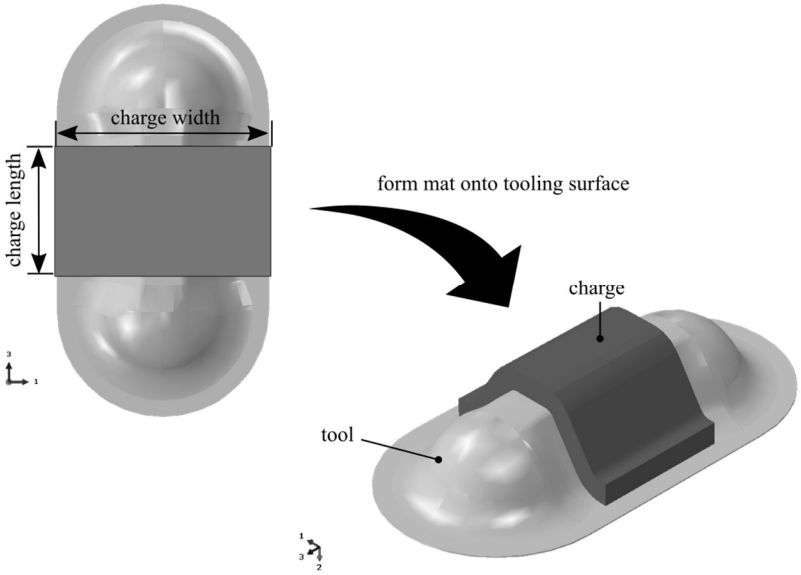

Figure 4: Diagram of Model Creating via Forming Type Operation of Charge

Following creation of the charge domains the orientation state must be initialized. As a simple method, the charge domains were segmented into five regions as shown in Figure 5 and each element was assigned an initial orientation vector generated from a planar uniform orientation distribution about the regional surface normal.

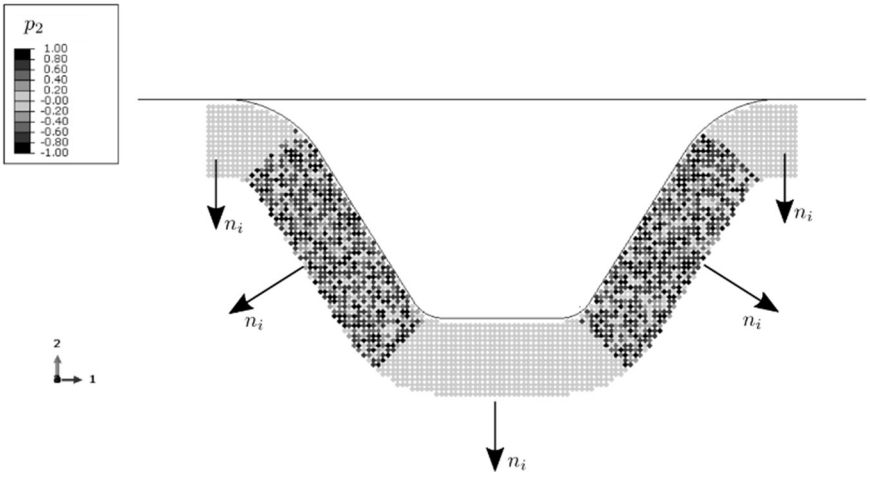

Figure 5: Regional Orientation Initialization Scheme

Experimental and Numerical Results

Experimental short shots were performed by shimming the double dome tool to six positions: 5 mm, 4 mm, 3 mm, 2 mm, 1 mm, and no shim. The full material charge was used in each case so that the conditions did not vary between trials other than the stopping position. In Figure 6, we show the results of the short shot experiment and flow simulation results at corresponding states.

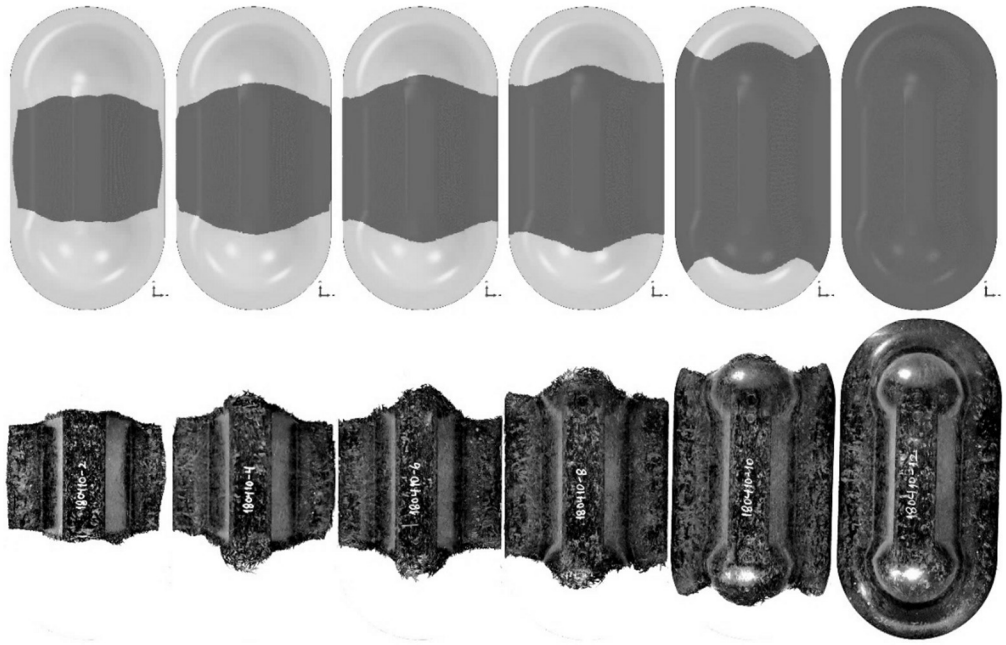

*Figure 6: Top View of Experimental Short Shots (bottom) and Simulated Flow Pattern (top) for **Transverse** Charge*

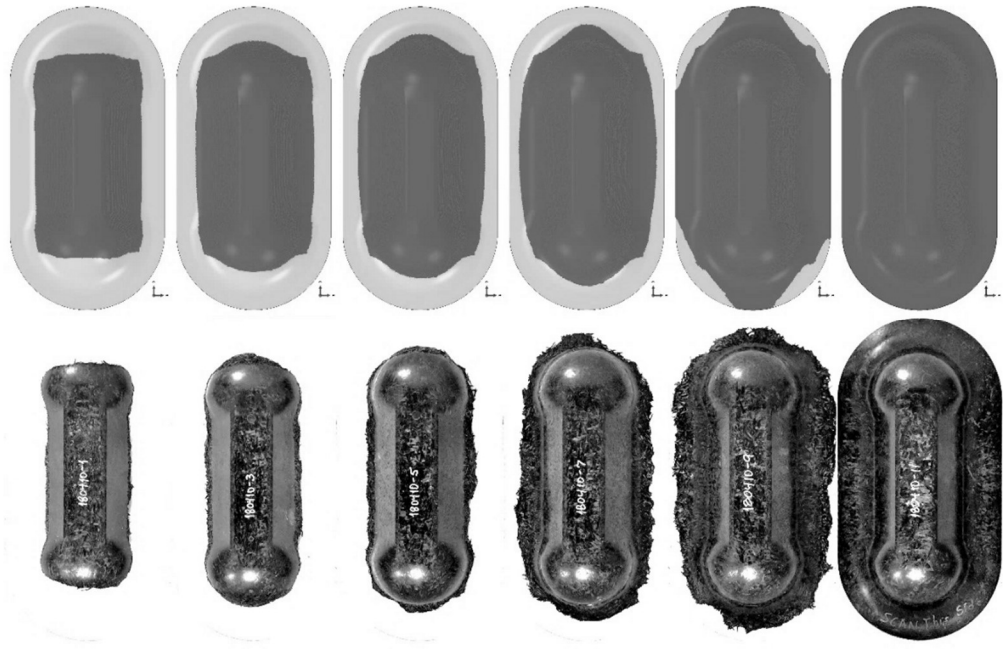

*Figure 7: Top View of Experimental Short Shots (bottom) and Simulated Flow Pattern (top) for **Axial** Charge*

Clearly, there is strong agreement between the predicted flow patterns and the short shots for the transverse charge. In this orientation, the charge initially flows similarly in all direction. However, the side boundary is encountered quite early in the total filling process; thus, the remainder of the flow proceeds as nearly one-dimensional flow, extending in the axial direction. Interestingly, the material near the side boundary flows faster than the rest of the charge and a knit line forms at the axial boundaries. The knit line can be seen clearly in the orientation structure shown in Figure 8 at both axial ends of the double dome, there are two regions of low A_{33} separated by a line of large A_{33} indicating that fibers are not crossing that line. Similarly, Figure 7 shows the flow pattern of the axial charge. The axial charge is sized and orientated so that the entire double dome fills relatively uniformly, in this case, the behavior is quite uninteresting. However, it must be noted that the initial charge of the simulation can be seen to be slightly too wide compared to the experiment. This source of this discrepancy arises from the charge domain creation technique. The formed surface was padded using the outward normal. While the formed surface had the correct width, the padding increased the average width of the charge. Again, this discrepancy was not correct as this work represents a blind prediction. The degree of alignment along the axial direction of the double dome can be seen in Figure 8.

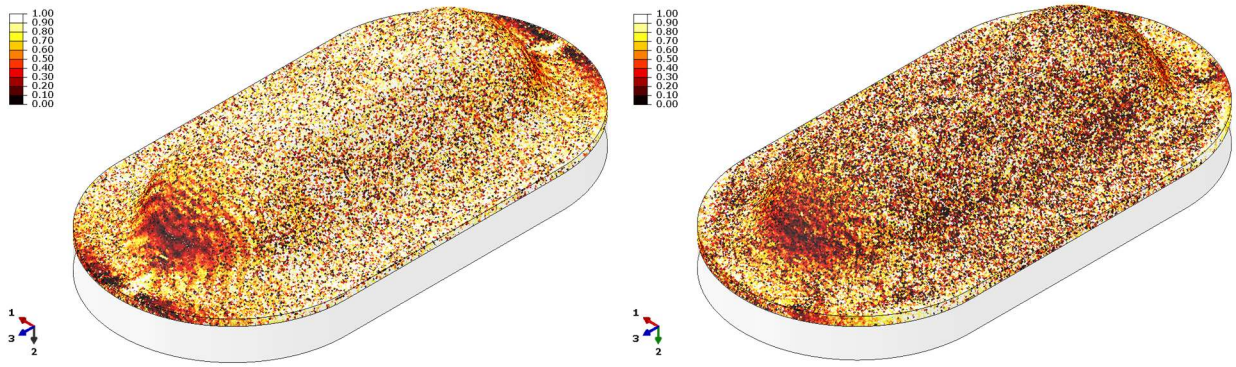

*Figure 8: Iso-View of Axial Degree of Alignment (A_{33}) for the **Transverse** Charge (left) and **Axial** Charge (right)*

To investigate the orientation state in the resulting simulations further, path plots were created which loosely correspond to the regions from which tensile bars could be excised from the double dome geometry. From a top view, a thin rectangular inspection region centered along the axial direction of the double dome and 150 mm long is swept along the x_1 direction. The average orientation tensor is then computed over the entire inspection region. The resulting orientation tensor components are plotted versus relative distance along the sweeping path. Figure 9 shows the orientation state variation for the transverse charge with the orientation tensor expressed in global coordinates. While this representation is direct, it is not particularly useful for interpretation as the orientation state in the slanted walls appears more complex than in reality. Therefore, in Figure 10 and Figure 11, the orientation tensor components of local orientation tensors are shown for the transverse charge model and axial charge model respectively, where the local orientation tensor, $\overline{\mathrm{A}}$, is determined using Equation (6) where n_i is the local surface normal.

$$\overline{\mathrm{A}} = \begin{bmatrix} \overline{\mathrm{A}}_{aa} & \overline{\mathrm{A}}_{at} & \overline{\mathrm{A}}_{an} \\ \overline{\mathrm{A}}_{at} & \overline{\mathrm{A}}_{tt} & \overline{\mathrm{A}}_{tn} \\ \overline{\mathrm{A}}_{an} & \overline{\mathrm{A}}_{tn} & \overline{\mathrm{A}}_{nn} \end{bmatrix} = \mathrm{R} \cdot \mathrm{A} \cdot \mathrm{R}^T, \qquad \mathrm{R} = \begin{bmatrix} 0 & 0 & 1 \\ n_2 & -n_1 & 0 \\ n_1 & n_2 & 0 \end{bmatrix} \tag{6}$$

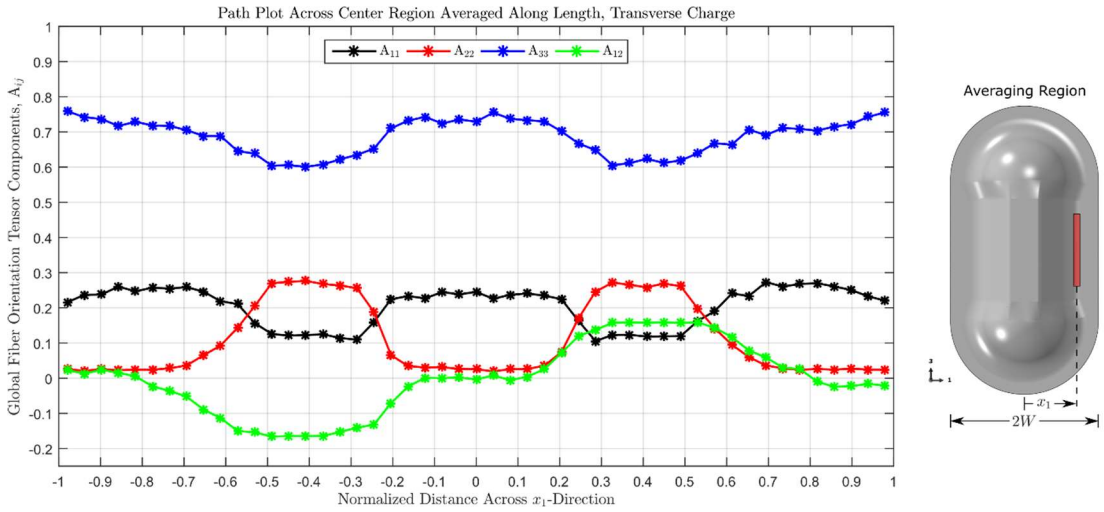

*Figure 9: Orientation State across Width of Double Dome for **Transverse** Charge in **Global** Coordinates*

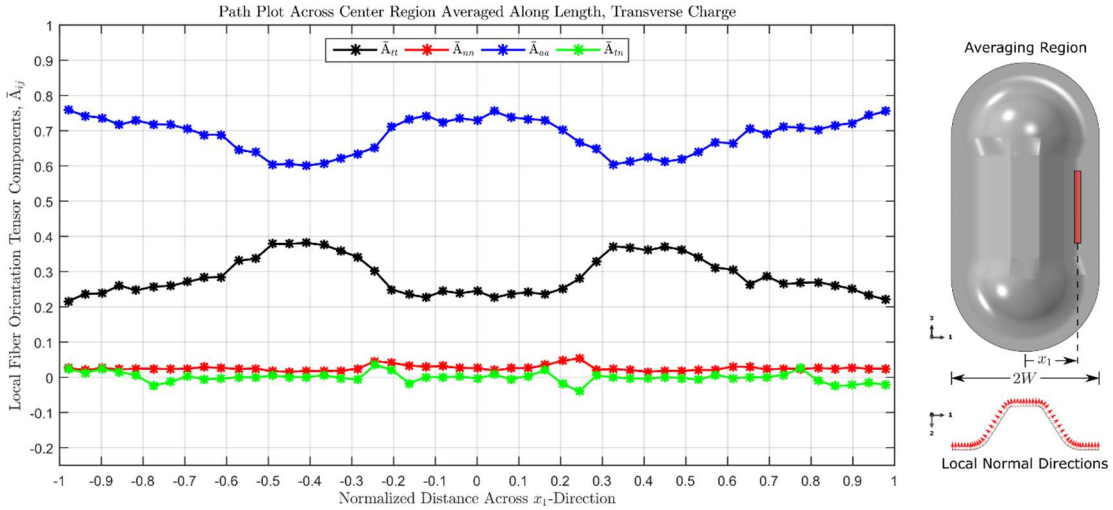

*Figure 10: Orientation State across Width of Double Dome for **Transverse** Charge in **Local** Coordinates*

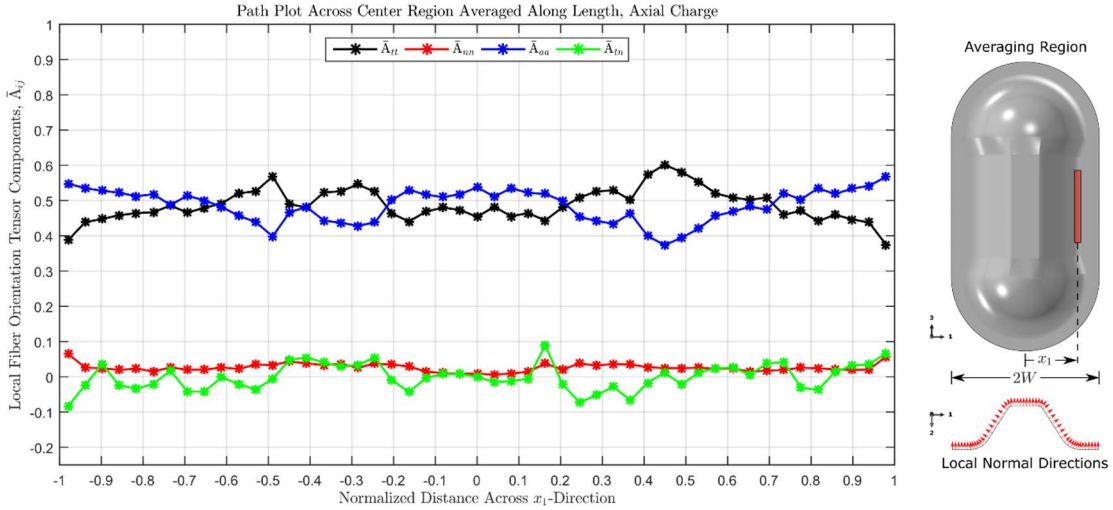

*Figure 11: Orientation State across Width of Double Dome for **Axial** Charge in **Local** Coordinates*

From Figure 10, we see that due to the one-dimension extension type flow encountered by the transverse charge the orientation state has been pulled towards axial alignment reaching an average degree of alignment of approximately $\mathrm{A}_{aa} = 0.7$. However, as the axial charge experienced two-dimensional extension throughout, the orientation state maintained approximately planar random. In both cases, the orientation state remained locally planar.

Conclusions

A simulation method for the flow and orientation analysis of prepreg platelet molding compounds, specifically a carbon fiber filled thermosetting materials used similarly to traditional SMC, has been presented. The method was limited by considering only essentially pristine molding conditions: isothermal conditions with uniform matrix viscosity through the domain and a molding time scale much less than the thermoset curing timescale. Nevertheless, the presented coupled fiber orientation and anisotropic viscosity approach implemented in Abaqus/Explicit using a VUMAT and taking advantage of the SPH solution method showed *predictive* results for flow patterns of two different charge configurations. The full simulation procedure involves charge domain creation, orientation initialization, and, finally, flow simulation. The investigation shows the large effect initial charge placement and charge orientation have on the flow pattern and resulting orientation state in the final part. Future work involves development of automated charge domain creation and orientation initialization using local surface normals rather than regional. These advancements are necessary so that the presented approach can be applied for more general and complex tool geometries and initial charge placements.

Acknowledgements

This work was sponsored by the Institute for Advanced Composites Manufacturing Innovation under Project 3.2. The authors wish to thank Jason Reese from Dow Chemical and Jeff Dahl from Ford Motor Company for performing the short shot experiments and Nate Sharp from Purdue University for performing the forming simulation used to initialize the axial charge.

Bibliography

[1] Pipes RB, McCullough RL, Taggart DG. Behavior of discontinuous fiber composites: Fiber orientation. Polym Compos 1982;3:34–9. doi:10.1002/pc.750030107.

[2] Papathanasiou TD, Guell DC. Flow-Induced Alignment in Composite Materials. Woodhead Publishing Limited; 1997. doi:10.1201/9781439822739.

[3] Favaloro AJ. Rheological Behavior and Manufacturing Simulation of Prepreg Platelet Molding Systems. Purdue University, 2017.

[4] Favaloro AJ, Sommer DE, Pipes RB. Anisotropic Viscous Flow Simulation for Fiber Orientation Analysis. Int. SAMPE Tech. Conf., 2017, p. 1486–96.

[5] Jeffery GB. The Motion of Ellipsoidal Particles Immersed in a Viscous Fluid. Proc R Soc A Math Phys Eng Sci 1922;102:161–79. doi:10.1098/rspa.1922.0078.

[6] Advani SG, Tucker CL. The Use of Tensors to Describe and Predict Fiber Orientation in Short Fiber Composites. J Rheol (N Y N Y) 1987;31:751–84. doi:10.1122/1.549945.

[7] Folgar F, Tucker CL. Orientation Behavior of Fibers in Concentrated Suspensions. J Reinf Plast Compos 1984;3:98–119. doi:10.1177/073168448400300201.

[8] Phelps JH, Tucker CL. An anisotropic rotary diffusion model for fiber orientation in short- and long-fiber thermoplastics. J Nonnewton Fluid Mech 2009;156:165–76. doi:10.1016/j.jnnfm.2008.08.002.

[9] Tseng H-C, Chang R-Y, Hsu C-H. An objective tensor to predict anisotropic fiber orientation in concentrated suspensions. J Rheol (N Y N Y) 2016;60:215–24. doi:10.1122/1.4939098.

[10] Tseng H-C, Chang R-Y, Hsu C-H. The use of principal spatial tensor to predict anisotropic fiber orientation in concentrated fiber suspensions. J Rheol (N Y N Y) 2018;62:313–20. doi:10.1122/1.4998520.

[11] Ericsson KA, Toll S, Manson J-AE. The two-way interaction between anisotropic flow and fiber orientation in squeeze flow. J Rheol (N Y N Y) 1997;41:491. doi:10.1122/1.550833.

[12] Sommer DE, Favaloro AJ, Pipes RB. Coupling anisotropic viscosity and fiber orientation in applications to squeeze flow. J Rheol (N Y N Y) 2018;62:669. doi:10.1122/1.5013098.

[13] Pipes RB, Coffin DW, Simacek P, Shuler SF, Okine RK. Rheological Behavior of Collimated Fiber Thermoplastic Composite Materials. Flow Rheol. Polym. Compos. Manuf., 1994, p. 85–125.

[14] Beaussart AJ, Hearle JWS, Pipes RB. Constitutive relationships for anisotropic viscous materials. Compos Sci Technol 1993;49:335–9. doi:10.1016/0266-3538(93)90064-N.

[15] Dumont P, Orgéas L, Le Corre S, Favier D. Anisotropic viscous behavior of sheet molding compounds (SMC) during compression molding. Int J Plast 2003;19:625–46. doi:10.1016/S0749-6419(01)00077-8.

[16] Barone MR, Caulk DA. Kinematics of flow in sheet molding compounds. Polym Compos 1985;6:105–9. doi:10.1002/pc.750060208.

[17] Barone MR, Caulk DA. A Model for the Flow of a Chopped Fiber Reinforced Polymer Compound in Compression Molding. J Appl Mech 1986;53:361. doi:10.1115/1.3171765.

[18] Tucker CL. Flow regimes for fiber suspensions in narrow gaps. J Nonnewton Fluid Mech 1991;39:239–68. doi:10.1016/0377-0257(91)80017-E.